The 3rd International Conference on
"Computational Mechanics
and Virtual Engineering"
COMEC 2009
29 – 30 OCTOBER 2009, Brasov, Romania

THE INFLUENCE OF FORCED STEERING VIBRATIONS ON A WHEEL AND DYNAMIC EFFECT OF A WHEEL WITH ABS BRAKING ON UNDULATED ROAD II

Vasii Marian[1]; Scutaru Maria Luminita[2]; Vlase Sorin[2]
[1]Renault Technologie Roumanie", Department Prestations Clients, marian.vasii-renexter@renaults.com
[2]Transilvania" University of Brasov-Romania, Department of Mechanics, luminitascutaru@yahoo.com, svlase@yahoo.com

***Abstract**: The aim of this section is to investigate the influence of dynamic effects due to vertical and longitudinal wheel vibrations excited by road irregularities upon the braking performance of the tyre and anti-lock braking system. These disturbing factors affect the angular velocity of the wheel and consequently may introduce disinformation in the signals transmitted to the ABS system upon which its proper functioning is based.*

***Keyword:** vibration, degrees of freedom, motion, wheel, brake*

1.INTRODUCTION

One may take the simple view that the primary function of the anti-lock device is to control the brake slip of the wheel to confine the wheel slip within a narrow range around the slip value at which the longitudinal tyre force peaks. In the same range it fortunately turns out that the lateral force that the tyre develops as a response to the wheel slip angle is usually sufficient to keep the vehicle stable and steer able.

In order to keep the treatment simple, we will restrict the vehicle motion to straight line braking and consider a quarter vehicle with wheel and axle that is suspended with respect to the vehicle body through a vertical and a longitudinal spring and damper. The analysis is based on the study of Van der Jagt et al.(1989).

2. IN-PLANE MODEL OF SUSPENSION AND WHEEL/TYRE ASSEMBLY

The vehicle is assumed to move along a straight line with speed V. The forward acceleration of the vehicle body is considered to be proportional with the longitudinal tyre force F_x. Vertical and horizontal vehicle body parasitic motions will be neglected with respect to those of the wheel axle. Consequently, the role of the wheel suspension is restricted to axle motion alone. These simplifications enable us to concentrate on the influence of the complex interactions between motions of the axle and the tyre upon the braking performance of the tyre. Figure 5 depicts the system to be studied. We have axle displacements x and z and a vertical road profile described by w and its slope dw/ds.

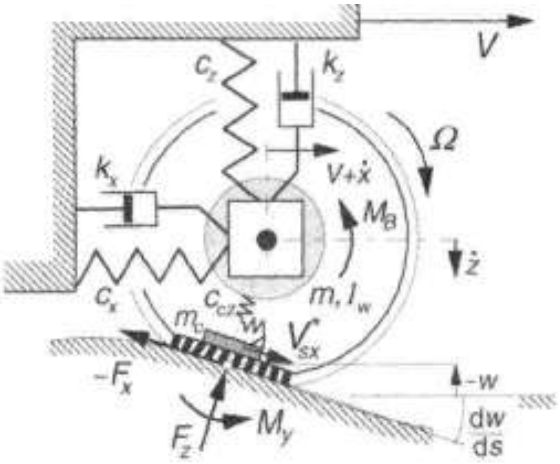

Figure 5: System configuration for the study of controlled braking on undulated road surface.

To suit the limitations of the tyre model employed, the wavelength λ of the road undulation is chosen relatively large. The wheel angular velocity is Ω and the braking torque is denoted with M_B. The unsprung mass and the polar moment of inertia of the wheel are lumped with a large part of those of the tyre and are denoted with m and I_w.

Through the tyre radial deflection the normal load is generated. Since we intend to consider possibly large slip forces, the analysis has to account for nonlinear tyre characteristic properties. The contact relaxation length σ_c will be disregarded here. In the model, a contact patch mass m_c is introduced that can move with respect to the wheel rim in tangential direction, thereby producing the longitudinal carcass deflection u. The contact patch mass may develop a slip speed with respect to the road denoted by V^*_{sx}. The transient slip is defined by (V>0):

$$k' = -\frac{V_{sx}}{V} \tag{21}$$

This longitudinal slip ratio is used as input in the steady-state longitudinal tyre characteristic. The internal tyre force that acts in the carcass and on the wheel axle will be designated as F_m while the tangential contact force is denoted with F_x. According to the theory, this slip force is governed by the steady-state force vs slip relationship $F_{xss}(K)$ which may be modelled with the *Magic Formula.*

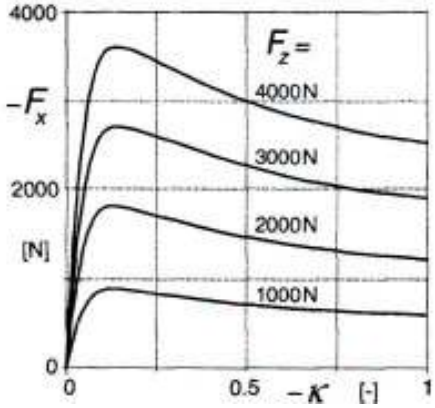

Figure 6: Steady-state tyre brake force characteristics at different loads as computed with the aid of the Magic Formula and the similarity technique.

Since we have to consider the influence of a varying normal load, the relationship must contain the dependency on F_z. We have the following equations:

$$F_{x,ss} = \frac{F_z}{F_{zo}} F_{xo}(k_{eq}) \tag{22}$$

with argument

$$(k_{eq}) = \frac{F_{zo}}{F_z} \frac{C_{Fk}(F_z)}{C_{Fko}} \tag{23}$$

The master characteristic $F_{XO(K)}$ described by the *Magic Formula* holds at the reference load F_{zo} which is taken equal to the average load. Its argument K is replaced by the equivalent slip value K_{eq}. Also the longitudinal slip stiffness C_{FKO} is defined at the reference load. In Fig.6 the steady-state force characteristics have been presented for a set of vertical loads.

2.1 In-plane braking dynamics equations

The system has as input the road profile w and the brake torque M_B. The level w and the forward slope dw/ds are given as sinusoidal functions of the travelled distance s. To partly linearise the equations, the road forward slope is assumed to be small. The brake torque ultimately results from a control algorithm but may in the present analysis be considered as a given function of time.

The following equations apply for the wheel rotational dynamics, the horizontal and vertical axle motions and the tangential motion of the contact patch mass:

$$I_w(\dot{\Omega} + rF_{xa} + M_Y = -M_B \quad \textbf{(24)}$$

$$m\ddot{x} + k_x\dot{x} + c_x x - F_{xo} - F_z\frac{dw}{ds} = 0 \quad \textbf{(25)}$$

$$m\ddot{z} + k_z\dot{z} + c_z z + F_z - F_{xo}\frac{dw}{ds} = 0 \quad \textbf{(26)}$$

$$m_c\dot{V}_{sx} + F_{xa} - F_x = 0 \quad \textbf{(27)}$$

with auxiliary equations for the tire loaded radius

$$r = r_0 - p \quad \textbf{(28)}$$

The radial deflection

$$p = z - w \quad \textbf{(29)}$$

The effective rolling radius

$$r_e = r_e(p) \quad \textbf{(30)}$$

The longitudinal carcass deflection rate

$$\dot{u} = V'_{sx} - V_{sx} \quad \textbf{(31)}$$

The wheel slip velocity

$$V_{sx} = V + \dot{x} - r_e\Omega + \dot{z}\frac{dw}{ds} \quad \textbf{(32)}$$

And the transient slip

$$k' = -\frac{V'_{sx}}{V} \quad \textbf{(33)}$$

Moreover ,the fooling constitutive relations are to be accounted for

$$F_z = F_z(p,u) \quad \textbf{(34)}$$

$$F_{xa} = F_{xa}(u,\dot{u}) \quad \textbf{(35)}$$

$$M_y = M_y(F_z,F_x) \quad \textbf{(36)}$$

$$F_x = F_{x,ss}(k',F_z) \quad \textbf{(37)}$$

The function (37) is represented by Eqs.(22) and illustrated in Figure 6. The remaining constitutive relations are simplified to linear expressions.

2.2 Frequency response of wheel speed to road unevenness

As essential element of the analysis we will assess the response of the wheel angular velocity variation to road undulations at a given constant brake torque.

For this, the set of equations may be linearised around a given point of operation characterized by the average load F_{z0}, the constant brake torque M_{Bo} and the average slip ratio K_0. We find for the constitutive relations:

$$\tilde{F}_z = c_{cz}(\tilde{p} + e_{zx}\tilde{u}) \quad \textbf{(38)}$$

$$\tilde{F}_{xa} = c_{cx}\tilde{u} + k_{cx}\dot{\tilde{u}} + e_{xz}\tilde{F}_z) \quad \textbf{(39)}$$

$$\tilde{M}_Y = A_r \tilde{F}_z + B_r \tilde{F}_{xa} \quad \textbf{(40)}$$

$$\tilde{F}_x = C_{xz} \tilde{F}_Z + C_{xk} \tilde{k}') \quad \textbf{(41)}$$

Where with the use of eqs 8.86,8,87

$$C_{xz} = \frac{\partial F_{x,ss}}{\partial F_z} = \frac{F_{xo}}{F_{zo}} + k_O \left(\frac{1}{C_{Fk0}} \frac{dC_{Fk}}{dF_z} - \frac{1}{F_{zo}}\right) \frac{dF_{xo}}{dk_{eq}} \quad \textbf{(42)}$$

And

$$C_{xz} = \frac{dF_{xo}}{dk_{eq}} \quad \textbf{(43)}$$

For the variation in effective rolling radius we have

$$\tilde{r}_e = -\eta \tilde{p} \quad \textbf{(44)}$$

The linearised equations of motion are obtained from the Eqs. (24--27) by subtracting the average, steady-state values of the variable quantities and neglect products of small variations.

The frequency response of Ω to w has been calculated for different values of the longitudinal suspension stiffness c_x. The average condition is given by: the vehicle speed V_0=60 km/h, a vertical load F_{zo} = 3000 N and a brake torque M_{Bo} = 300 Nm that corresponds to an average slip ratio κ_0 = -0.021. The road undulation amplitude $\hat{w} = 0{,}001m$

Some of the tyre constitutive relations were determined directly from measurements while for some of the parameters values have been estimated. The small interaction parameters, $\eta, e_{xz},$ and e_{zx} and also the rolling resistance parameters A_r and B_r have been disregarded. Table 8.3 lists the parameter values used in the computations.

I_w	0.95 kgm^2	c_x	100 kN/m	c_z	20kN/m	F_{zo}	3000 N
m	35 kg	k_x	2 kNs/m	k_z	2 kNs/m	r_o	0.29 m
m_c	1 kg	c_{cx}	10^3 kN/m	c_{cz}	170 kN/m	k_{cx}	0.8 kNs/m

Table 2. Parameter values for wheel/tire/ suspension system

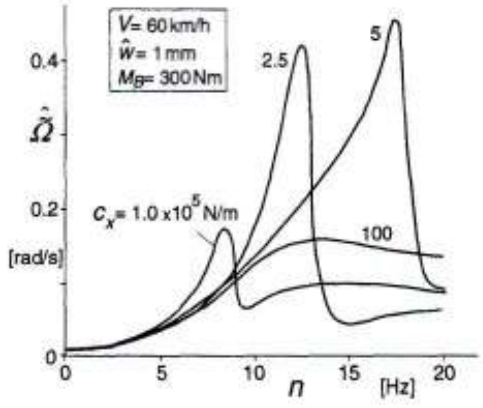

Figure 7: Frequency response of amplitude of wheel spin fluctuations to road undulations w at a constant speed Kand brake torque M_B and for different values of the longitudinal suspension stiffness c_x.

Figure 7 displays the amplitude of the wheel angular velocity variation as a function of the imposed frequency that is inversely proportional with the wavelength of the undulation. It is seen that the resonance peak height and the resonance frequency strongly depend on the fore and aft suspension stiffness.

3. ANTI-LOCK BRAKING ALGORITHM AND SIMULATION

The actual control algorithms of ABS devices marketed by manufacturers can be quite complex and are proprietary items which incorporate several practical considerations. However, almost all algorithms make use of raw data pertaining to the angular speed and acceleration of the wheels. A detailed discussion of the various algorithms for predicting wheel motions and modulating the brake torque accordingly, has been given by Guntur (1975). The operational characteristic of a control algorithm used here for the purpose of illustration is shown in Fig.8. The salient features of the criteria used to increase or decrease applied brake torque (pressure) during a braking cycle depend critically upon both the momentary and threshold values of Ω and of $\dot{\Omega}$. It is assumed that the brake torque rate can be controlled at three different levels. Upon application of the brake the torque rises at a constant rate until point B is reached. After that the torque is reduced linearly until point C. The brake torque remains constant in the interval between points C and E. Compound criteria are considered at points A and B for predicting when braking should be reduced to prevent the wheel from locking. Thus we have from the starting of brake application: Increase of torque for $0 < t < t_B$ according to: $dM_B/dt = R_x$ The preliminary prediction time t_A is given by:

$$r_{eo}\dot{\Omega}(t_A) = T_g$$

where r_{eo} stands for the nominal effective rolling radius and T for a constant which sets the treshold for $\dot{\Omega}$. From time t_B we have:

Decrease of torque for $t_B<t<t_c$ according to: $dM_B/dt = R_2$

The instant of prediction and action t_B is defined by:

$$r_{eo}\{\Omega(t_A) - \Omega(t_B)\} - T_g(t_B - t_A) = \Delta V_B$$

The time t_c marks the beginning of the constant torque phase CE, i.e.:

Constant torque for $t_c<t<t_E$: $dM_B/dt = 0$ Time t_c is found from:

$$\Omega(t_c) = 0$$

Similarly, the criterion for increasing the torque at E:

Increase of torque for $t > t_E$ according to: $dM_B / dt = R_1$ is given by the compound reselection conditions generated at points D and E, with t_D and t_E being found from:

$$\ddot{\Omega}(t_D) = 0$$

and

$$r_{eo}\{\Omega(t_D) - \Omega(t_E)\} + \dot{\Omega}(t_D)(t_E - t_D) = \Delta V_E$$

For the simulation the following values have been used:

T= -1, $\Delta V_B = 0.1 r_{eo}\Omega(t_B)$

and $\Delta V_E = 1m/s$ The brake torque rates have been set to:

R_x=-R_2= 19000 Nm/s

In order to simulate the braking man oeuvre of a quarter vehicle equipped with the anti-lock braking system, the deceleration of the vehicle is taken to be proportional to F_x. The results of the simulations performed are presented in Fig.9. The left-hand diagrams refer to the case of braking on an ideally flat road while the diagrams on the right-hand side depict the results obtained with the same system on a wavy road surface. For the purpose of simulation, the model was extended to include a hydraulic sub-system interposed between the brake pedal and the wheel cylinder. However, this extension is not essential to our discussion. In both cases the same hydraulic sub-system was used and the same control algorithm as the one discussed above was implemented.

The further parameters used in the simulation were: Initial speed of the vehicle: 60km/h, the road input with a wavelength of 0.83 m and an amplitude of 0.005 m.

4. CONCLUSION

The results of the simulation show that brake slip variations occur both on a flat as well as on undulated road surfaces. However, the very large variations of the transient slip value κ' in the latter case lead to a further deterioration of the braking performance. The average vehicle deceleration drops down from 7.1 m/s^2 to approximately 6 m/s^2. Although large fluctuations in the vertical tyre force are mainly responsible for this reduction, it is equally clear that severe perturbation occurring both in Ω and $\dot{\Omega}$ may be an additional source of misinformation for the anti-lock control algorithm The important reduction in braking effectiveness resulting from vertical tyre force variations may be attributed to the term $\boldsymbol{C}_{cz}$ in the linearised constitutive relation (42) of the rolling and slipping tyre, and in particular to the contribution of the variation of the longitudinal slip stiffness with wheel load dC_F/dF_z. Both vertical and horizontal vibrations of the axle and the vertical load fluctuations on wavy roads appear to adversely influence the braking performance of the tyre as well as that of the anti-lock system.

In 1986, Tanguy made a preliminary study of such effects using a different control algorithm. He pointed out that wheel vibrations on uneven roads can pose serious problems of misinformation for the control logic of the anti-lock system. The results of the simulations discussed above and reported by Van der Jagt (1989) confirm Tanguy's findings.

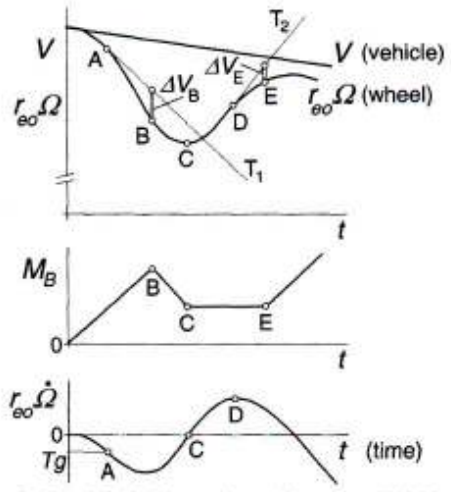

Figure 8
Example of an ABS algorithm used to modulate the applied brake torque

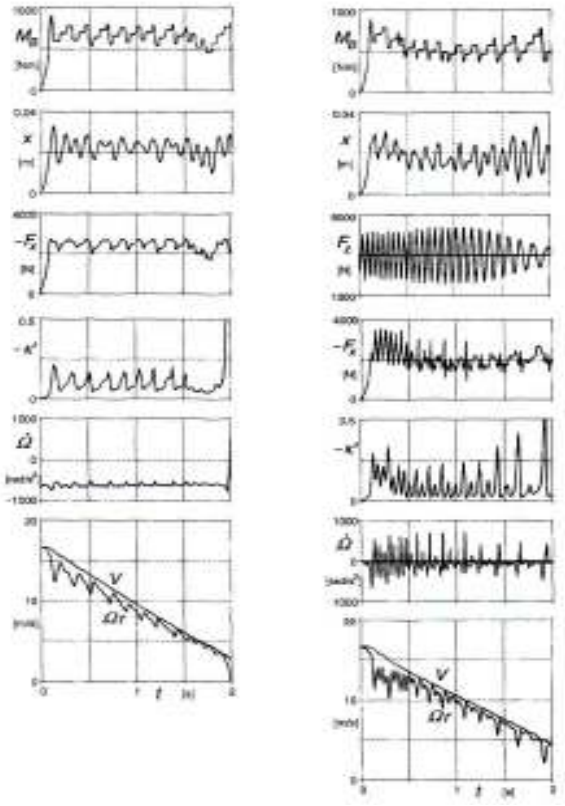

Figure 9:
Left: Simulation of braking with ABS on an ideally flat road
Right: Simulation of braking with ABS on a wavy road.

REFERENCES

[1] Badalamenti, J.M., and Doyle, G.R. (1988): Radial-interradial spring tire models. J. *of Vibration, Acoustic, Stress and Reliability in Design,* 110, 1, 1988.

[2] Bakker, E., Pacejka, H.B., and Lidner, L. (1989): A New Tire Model with an Application in Vehicle Dynamics Studies. *SAE Paper* No. 890087, 1989.

[3] Bandel, P., and Monguzzi, C. (1988): Simulation model of the dynamic behavior of a tire running over an obstacle. *Tire Science and Technology,* TSTCA, 16, 2, 1988.

[4] Bandel, P., and Bernardo, C. di (1989): A Test for Measuring Transient Characteristics of Tires. *Tire Science and Technology,* 17, 2, 1989.

[4] Bayer, B. (1988): Flattern und Pendeln bei Kraftr~idern. *Automobil lndustrie,* 2, 1988.

[5] Bayle, P., Forissier, J.F., and Lafon, S. (1993): A New Tyre Model for Vehicle Dynamics Simulation. *Automotive Technology International,* 1993.

[6] Bernard, J.E., Segel, L., and Wild, R.E. (1977): Tire shear force generation during combined steering and braking maneuvres. *SAE Paper* 770852, 1977.

[7] Berritta, R., Biral, F., and Garbin, S. (2000): Evaluation of motorcycle handling and multibody modelling and simulation. In: *Proceedings of 6 th Int. Conference on HighTech. Engines and Cars,* Modena, 2000.

[8] Berzeri, M., and Maurice, J.P. (1996): A mathematical model for studying the out-of plane behaviour of a pneumatic tyre under several kinematic conditions. FISITA Youth Congress, Prague, June 1996.

[9] Besselink, I.J.M. (2000): *Shimmy of Aircraft Main Landing Gears.* Dissertation, TU Delft, 2000.

[10] Biral, F., and Da Lio, M. (2001): Modelling drivers with the optimal maneuver method. In: *Proceedings of ATA 2001,* The Role of Experiments in the Automotive Product Development Process, Florence, 2001.

[11] B6hm, F. (1963): Der Rollvorgang des Automobil-Rades. *ZAMM* 43, T56-T60, 1963.

[12] Borgmann, W. (1963): *Theoretische und experimentelle Untersuchungen an Luftreifen bei Schriiglauf.* Dissertation, Braunschweig, 1963.

[13] Breuer, T., and Pruckner, A. (1998): Advanced dynamic motorbike analysis and driver simulation. In: *13 th European ADAMS Users' Conference,* Paris, 1998.
[14] Brockman, R.A., and Braisted, W.R. (1994): Critical Speed Estimation of Aircraft Tires. *Tire Science and Technology,* 22, 2, 1994.
[15] Br6der, K., Haardt, H., and Paul, U. (1973): Reifenprtifstand mit innerer und ~iusserer Fahrbahn. ATZ, Vol. 75 (1973), No. 2.
[16] Bruni, S., Cheli, F., and Resta, F. (1996): On the identification in time domain of the parameters of a tyre model for the study of in-plane dynamics. In: *Proceedings of 2 "d Colloquium on Tyre Models for Vehicle Analysis,* eds. F.B6hm and H.P.Willumeit,
[17] Berlin 1997, Suppl. Vehicle System Dynamics, 27, 1996. CCG (2004): Tyre Models for Vehicle Dynamics Simulation. *Seminar TV4.08 Lecture notes,* Coord. P.Lugner, Vienna, Sept. 1-2, 2004, Carl Cranz Gesellschaft, 82234 Oberpfaffenhofen, Germany.